

MEMBRANE BASED EVAPORATION CRYSTALLIZATION

A. König, D. Weckesser

Dept. of Separation Science & Technology, University of Erlangen,

D-91058 Erlangen, Germany

axel.koenig@cbi.uni-erlangen.de

Well-controlled crystallization is the best method for preparing materials that are uniform in shape, size, structure and purity. Crystal growth as well as nucleation depends on supersaturation degree. The local gradient of supersaturation sometimes acts as a limiting factor in respect to uniformity of the product quality. The aim of this work is to introduce an innovative methodology – the membrane crystallization – to control the generation of supersaturation. The transmembrane distillation (TMD) of water from saturated solution based on hydrophobic micro porous membranes was used to reach supersaturation in the crystallization of NaCl from aqueous solutions. Vapour pressure gradient is the driving force for the operation. The experiments were carried out in a laboratory plant for investigating the effect of the mass transfer rate as a function of the retention time, slurry density, temperature and supersaturation level of the solution. The crystallization rates obtained were then compared with the ones by simulation of the process.

1. Introduction

Crystallization operates according to the local gradient and the dynamics of generating supersaturation as source and degeneration supersaturation by growth and nucleation as drain. Crystal modification, shape, size and purity depend strongly on the level of local supersaturation. High level of supersaturation often causes unstable modifications, needle like shape, small and impure crystals. Controlling the supersaturation can be essential to reduce this problem.

Membranes are an interesting tool to control and to limit the mass transfer and therefore – in combination with crystallization – the maximum level of supersaturation.

Walton et al. has already successfully used membranes 100 years ago preparing inorganic and organic crystals from solutions by controlling the mass transfer of water through the semi-permeable membranes of different materials [WAL09]. In later times the concentration of salt solutions by membrane distillation (MD) with the aim of producing drinking water and salt as by-product was investigated [SCH84, GRY02]. Softening of drinking water by ultrafiltration in combination with seeding of crystals (mainly CaSO_4 or CaCO_3) is a common technology of membrane based crystallization [KÜM87]. Curcio et al. have investigated membrane crystallization of sodium chloride [CUR01] as well as of organic products such as lysozyme [CUR03].

Membrane distillation is a recent process framed in the most general class of membrane contactors, an emerging technology in which the membrane promotes the mass transfer operation acting not as a selective barrier but accomplishing the separation on the principle of phase equilibria. The crucial part of the technology is the stability of the vapour-liquid interface on one site of the membrane only. Hydrophobic conditions of micro porous membranes are guaranteed for materials such as Polypropylene PP and Teflon PTFE.

The mass transfer rate of MD is limited by concentration and temperature of the solution, polarisation phenomena, by mass and heat transfer resistance of the membrane, and the boundary layer adjustment. Several techniques exist, depending on the method used to recover the vapour once it has migrated along the membrane. The main advantages of TMD are the total rejection of ions and other nonvolatiles, the low operating temperatures, the low energy requirements and the reduced global size. Furthermore the precise control and gentle operation generating supersaturation is an other important characteristic.

2. Experimental Section

A schematic representation of the experimental setup is depicted in Figure 1. The setup consists of two cycles. The flow of the saturated salt suspension is circulated in cycle 1, whereas the sweeping gas is circulated in cycle 2. In the evaporator (membrane module) the two flows converge in a counter current way and the water is evaporated transmembrane. In the module, the suspension is induced tube side and the sweep gas shell side. The water vapour is assimilated by the sweeping gas and condensed out in the trap in order to measure the amount of evaporated water. Then the unloaded sweeping gas is re-circulated to the membrane module. Crystallization occurs in the crystallizer. Two types of crystallizers are used: Crystallizer one operates as mixed suspension mixed product removal (MSMPR) and crystallizer two as classified product removal (CPR). The separation step consists of a filter centrifuge returning mother liquor M and crystallite C as final products.

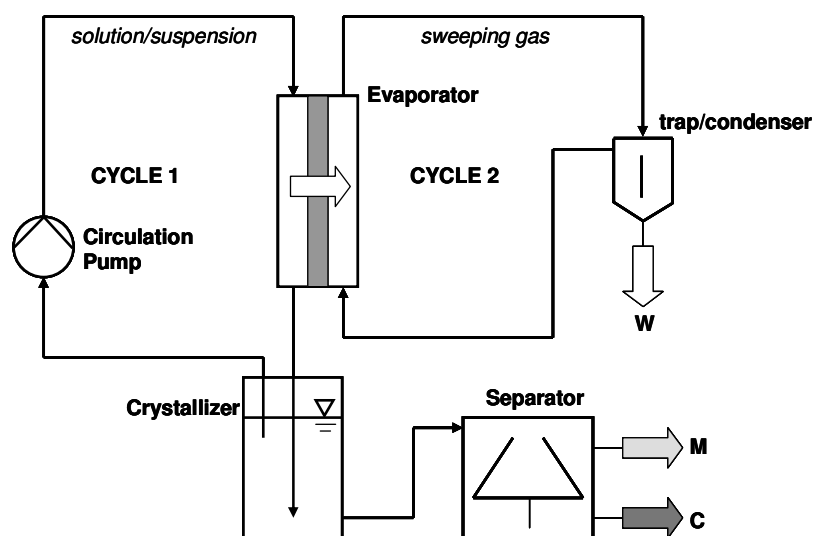


Figure 1: Schematic representation of the membrane based crystallization setup

The membrane based crystallization is carried out in batch mode. Transmembrane evaporated water W is measured continuously by weighting, while the mass of the crystallite C is measured by weighting after the end of the experiment.

To prevent heat losses, the membrane module and the temperature measuring probes are insulated. During an experiment the temperatures of the suspension and the sweeping gas at the inlet and the outlet of the module are measured continuously using Pt-1000 sensors.

The experiments are performed under several operating conditions with varying temperature of the suspension and varying volume flow rates of suspension and sweeping gas.

The main characteristics of the membrane module and the used membranes are specified in Table 1.

Table 1: Characteristics of the membrane module and the used membranes

Denotation	Abbreviation	Dimension	Value
membrane material	-	-	PP
membrane type	-	-	capillary
number of capillaries	N	-	21
available membrane area	A_M	m ²	0,0146
nominal pore size	d_{pore}	μm	0,2
membrane thickness	δ_M	μm	450
inner diameter of capillaries	d_i	μm	1800
outer diameter of capillaries	d_a	μm	2700
porosity	ε	-	0,6
tortuosity	τ	-	1

3. Mathematical Relationships

Regarding the membrane based distillation and crystallization, the material balance and the energy balance are coupled in a system of differential equations. The following equation describes the material balance across the membrane module for a differential surface area element dA_M/dz of the sweeping gas side according to the length of the module z and thus stands for the generation of supersaturation:

$$\frac{\partial^2 n_{tr}}{\partial t \cdot \partial z} = k_n \cdot \frac{\partial A_M}{\partial z} \cdot \varepsilon \cdot (p_w^s - p_w^{SG}) \quad (1)$$

The energy balance across the membrane is divided into two terms; a convective term and a heat conduction term:

$$\frac{\partial^2 q_{tr}}{\partial t \cdot \partial z} = \frac{\partial(\dot{m}_{tr} \cdot c_p \cdot T_s)}{\partial z} + k_q \cdot \frac{\partial A_M}{\partial z} \cdot (1 - \varepsilon) \cdot (T_s - T_{SG}) \quad (2)$$

The heat that is removed from the suspension side is introduced in the system as:

$$\frac{\partial^2 q_{Susp}}{\partial t \cdot \partial z} = -\Delta_v h \cdot \frac{\partial^2 n_{tr}}{\partial t \cdot \partial z} \cdot M_w - \frac{\partial(\dot{m}_{tr} \cdot c_{p,D} \cdot T_s)}{\partial z} - k_q \cdot \frac{\partial A_M}{\partial z} \cdot (1 - \varepsilon) \cdot (T_s - T_{SG}) \quad (3)$$

For the degradation of the supersaturation common crystal kinetic equations of nucleation and crystal growth are used. The nucleation rate B^0 is:

$$B^0 = k_B \cdot \Delta S^b \cdot M_D^j \cdot \varepsilon_{diss}^k \quad (4)$$

The crystal growth rate G is:

$$G = \frac{dL}{dt} = k_G \cdot S^g \quad (5)$$

4. Results and Discussion

The supersaturation is generated by evaporating water in the membrane module. Figure 2 shows the mass of water m_w evaporated across the membrane in dependence of the experimental time t_v for three different temperatures ($T_s=30$ °C, $T_s=35$ °C, $T_s=40$ °C) of the circulated suspension.

Each run takes experimental times of $t_v=7-9$ h to complete. During this time the transmembrane evaporated water increases linearly with time having regression coefficients of $R^2>0,99$. This means the evaporation rate of water remains constant throughout the run.

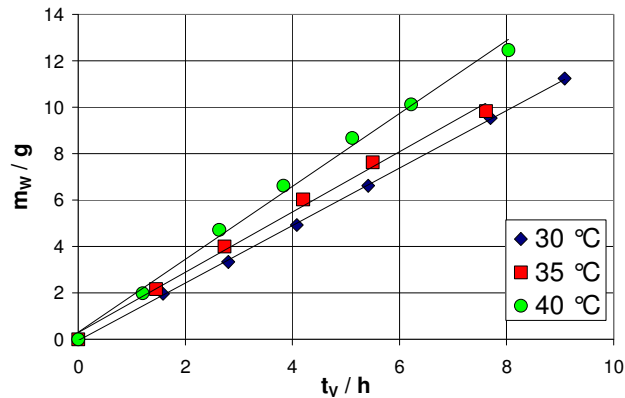


Figure 2: Mass of transmembrane evaporated water in dependence of the experimental time

The higher the temperature, the higher is the evaporation rate in the measured temperature range of the suspension between $T_s=30$ °C and $T_s=40$ °C. With an increasing temperature the partial water vapour pressure of the solution increases and thus the driving force across the membrane becomes larger with respect to constant evaporation enthalpy.

The mass of evaporated water is in good correspondence with the mass of produced salt in all experiments. The factor between the mass of produced salt and the mass of evaporated water (supersaturation loading of water with salt) keeps constant by varying operation parameters.

In the membrane crystallization experiments specific transport coefficients of water of $K_{tr}=2,0-3,3$ kg/m²hbar are determined, whereas the specific production coefficients of salt comprise $K_s=0,5-1,0$ kg/m²hbar. The ranges for $K_{tr/s}$ are depending on fluid dynamics only.

Experimental results of the specific transport coefficients of the transmembrane water flux are compared with the literature of Sweeping Gas MD (SGMD) and Direct Contact MD (DCMD). Gryta et al. [GRY02a] reports specific water transport coefficients of $K_{tr}=30-40$ kg/m²hbar in a DCMD-setup. These are ten times higher when compared to measured values in the present work. Also a comparison of the experimental results of Khayet et al. [KHA03], who uses a SGMD-setup, tends to higher specific water transport coefficients of $K_{tr}=40-60$ kg/m²hbar. In contrast, the values of $K_{tr}=3,0-5,0$ kg/m²hbar obtained from former own experiments of SGMD with water/ethanol-solutions are in good agreement. Calculated values based on the used experimental parameters also vary in between a range of $K_{tr}=2,0-6,0$ kg/m²hbar.

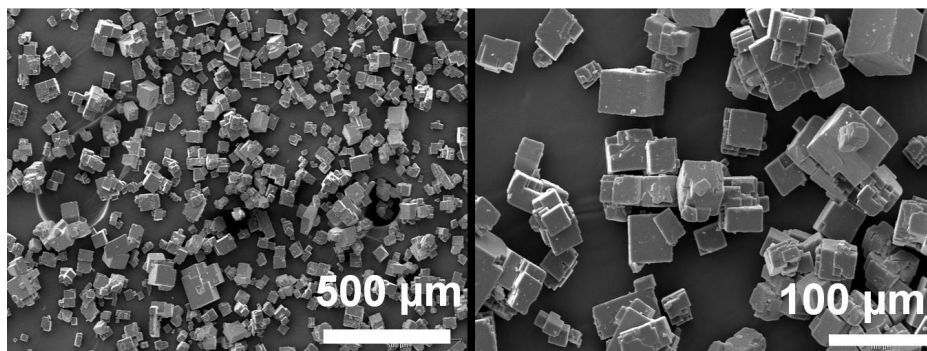


Figure 3: REM-micrographs of the produced NaCl crystals

In Figure 3 NaCl crystals produced in the present membrane based crystallization setup are presented showing the characteristic well-formed cubic shape. Besides single crystals, also agglomeration and aggregation in combination were observed.

A representative cumulative particle size distribution (PSD) is shown in Figure 4. The mean crystal diameter is $L_{50}=43 \mu\text{m}$, the maximum crystal size is $L_{\text{max}}=95 \mu\text{m}$ and the minimal crystal size is $L_{\text{min}}=24 \mu\text{m}$. Other PSDs show similar results at different operating conditions with respect to the temperature of the suspension and the volume flow rates of the suspension and the sweeping gas respectively.

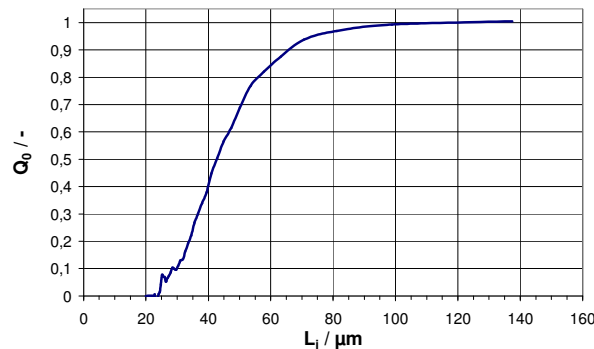


Figure 4: Representative particle size distribution of the produced NaCl crystals

Relatively small mean crystal sizes obtained in the experiments are due to the milling effect of the toothed wheel pump used for circulating the suspension. The purpose of using this kind of pump is to generate small crystals what means a high crystal area for degradation of the supersaturation. This consequently has a positive effect on preventing scaling in the membrane module on the one hand and blocking of the capillaries with crystals on the other hand. A certain amount of large crystals in the size range of $L=70\text{-}100 \mu\text{m}$ is attributed to the crystal growth, whereas in the small crystal size range no particles smaller than $L=20 \mu\text{m}$ are detected.

During the experimental runs the PSD remains constant and this also is owing to the used pump, because the growth of circulated crystal in the suspension is limited. Compared to Curcio et al. the CV-Values of the PSDs obtained within the present work are with $CV=25\text{-}35\%$ much lower. Curcio et al. report values of $CV=42\text{-}57\%$ [CUR01].

The modelling and simulation are based on the mathematical relations mentioned above and consist of modelling the generation of supersaturation in the membrane module on the one

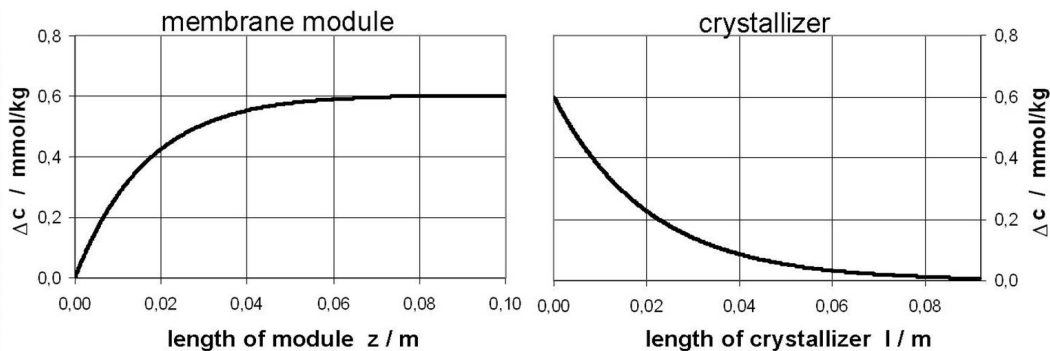


Figure 5: Simulated supersaturation profile along the membrane module (left) and in the crystallizer (right) for an experiment with the following parameters: $T_S=38 \text{ }^\circ\text{C}$, $T_{SG}=24 \text{ }^\circ\text{C}$, $\dot{V}_S=8,5 \cdot 10^{-6} \text{ m}^3/\text{s}$, $\dot{V}_{SG}=40 \cdot 10^{-6} \text{ m}^3/\text{s}$, $p_{SG,in}=670 \text{ Pa}$, $\bar{L}=40 \mu\text{m}$, $\dot{m}_W=2,67 \cdot 10^{-3} \text{ kg/h}$, $V_R=180 \cdot 10^{-6} \text{ m}^3$, $M_D=15 \text{ kg/m}^3$

hand and the degradation of supersaturation in the module, the crystallizer and the adjacent system on the other hand.

Figure 5 presents a simulated supersaturation profile based on modelling as shown in section 3. In the membrane module the supersaturation is established. A steep incline of the curve in the first part of the module gets flat with the module coordinate z and reaches a plateau at half way of the module. This profile directly corresponds with the evaporation rate along the module. The sweeping gas assimilates the transmembrane water vapour and already is saturated after half the module length. As in the module the saturation just is built up, in the crystallizer the complete saturation is degraded. No crystallization occurs in the module. This denotes that enough area for crystallization is provided to the system assuming that a constant mean crystal size in the suspension is circulated around the evaporator.

5. Conclusion

In this work the membrane based crystallization is employed to produce NaCl crystals from supersaturated aqueous solutions as model system. The task is feasible within experimental durations up to 9 h without transport-limiting effects. The obtained crystallization rates are reproducible and correspond directly with the measured evaporation rates. Typically cubic-shaped NaCl-crystals are produced. First simulations show that the supersaturation is generated in the membrane module and mainly completely degenerated in the crystallizer, whereas the mean crystal size remains constant when circulating a suspension around the module. Following tasks consist of transferring the obtained results and interrelations to other systems of substances with concerted manipulation of the crystal characteristics. Furthermore, the membrane based crystallization is applied for anti-solvent crystallization as well as for precipitation based on the principles of controlled mass transfer.

6. Nomenclature

n_{tr}	transmembrane water amount	mole	L	crystal size	μm
q_{tr}	transmembrane heat	J	M_D	Magma Density	kg/m^3
\dot{V}	volume flow rate	m^3/s	CV	coefficient of variation	%
\dot{m}	mass flow rate	kg/h	K_{tr}	specific transport coefficient of water	$\text{kg}/\text{m}^2\text{hbar}$
T	temperature	$^{\circ}\text{C}$	K_S	specific production coefficient of salt	$\text{kg}/\text{m}^2\text{hbar}$
p	pressure	Pa	ϵ_{diss}	energy of dissipation	J
c_p	specific heat capacity	$\text{J}/\text{g}\cdot\text{K}$	k_n	transport coefficient material	m/s
B^0	Nucleation rate	$\#/\text{m}^3\text{s}$	k_q	transport coefficient heat	$\text{W}/\text{m}^2\text{K}$
k_B	kinetic coefficient nucleation	-	ΔS	supersaturation	-
G	Growth rate	m/s	S	solution/suspension	
k_G	kinetic coefficient growth	-	SG	sweeping gas	
\bar{L}	mean crystal size	μm	Susp	suspension	

7. References

- [CUR01] CURCIO, E.; CRISCUOLI, A.; DRIOLI, E.: *Ind. Eng. Chem. Res.*, **40** (2001), p. 2679-2684
 [CUR03] CURCIO, E.; DI PROFIO, G.; DRIOLI, E.: *Journal of Crystal Growth*, **247** (2003), p. 166-176
 [GRY02] GRYTA, M.: *Chem. Pap.*, **56** (2002), 1, p. 14-19
 [GRY02a] GRYTA, M.: *Separation Science and Technology*, **37** (2002), 15, p. 3535-3558
 [KHA03] KHAYET, M.: *Desalination*, **157** (2003), 1-3, p. 297-305
 [KÜM97] KÜMMEL, R.; HOFFMANN, A.: *Chem.-Ing.-Tech.*, **69** (1997), p. 831-833
 [SCH84] SCHNEIDER, K.; VAN GASSEL, T. J.: *Chem.-Ing. Tech.*, **56** (1984), 7, p. 514-521
 [WAL09] WALTON, J. H., Jr.: *Journal of Physical Chemistry*, **13** (1909), p. 490-500